

# Variational Transformer: A Framework Beyond the Trade-off between Accuracy and Diversity for Image Captioning

Longzhen Yang, Shaohua Shang, Yihang Liu, Yitao Peng, Lianghua He\*

College of Electronic and Information Engineering

Tongji University

4800 Cao'an Highway, Shanghai, China 201804

{yanglongzhen, shaohuashang, 2111131, 2111132, helianghua}@tongji.edu.cn

## Abstract

Accuracy and Diversity are two essential metrizable manifestations in generating natural and semantically correct captions. Many efforts have been made to enhance one of them with another decayed due to the trade-off gap. However, compromise does not make the progress. Decayed diversity makes the captioner a repeater, and decayed accuracy makes it a fake advisor. In this work, we exploit a novel Variational Transformer framework to improve accuracy and diversity simultaneously. To ensure accuracy, we introduce the "Invisible Information Prior" along with the "Auto-selectable GMM" to instruct the encoder to learn the precise language information and object relation in different scenes. To ensure diversity, we propose the "Range-Median Reward" baseline to retain more diverse candidates with higher rewards during the RL-based training process. Experiments show that our method achieves the simultaneous promotion of accuracy (CIDEr) and diversity (self-CIDEr), up to 1.1 and 4.8 percent, compared with the baseline. Also, our method outperforms others under the newly proposed measurement of the trade-off gap, with at least 3.55 percent promotion.

## 1 Introduction

Generating diverse and accurate captions is a challenging task in image captioning and has not been accomplished yet, despite best efforts.

Though, recent method in [1] did achieve close numerical results to human ground truths (leave-one-out [2]) in both accuracy and diversity, the qualitative results can not be saying good ones, as shown in Figure 1. Note that the average human leave-one-out [3] performance in accuracy (CIDEr) is only 87.8, while current top scores of machine learning models are up to 130 at least. It is reasonable for human captions with good semantic structures known to get this low metric result due to diverse descriptions. However, for machine-learning-based works, it is hard to reveal the true semantic performance with low accuracy. On the other hand, common metrics proposed to capture diversity involve no accuracy mea-

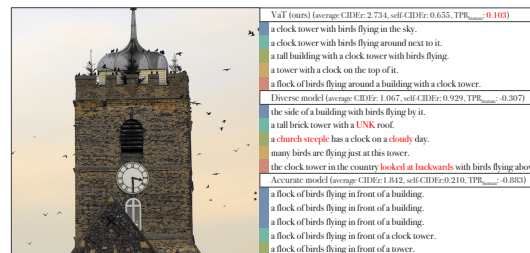


Figure 1: Captions generated from different models. 1) We use CIDEr and self-CIDEr to present the performance of accuracy and diversity, respectively. We denote distinct captions with different colors. 2) Good diverse generations should be established on the solid accuracy performance.

sure [4], thus, can be misleading with wrong words to manifest inflating diversity scores. Therefore, we suppose that the diverse generation should be dependent on the accuracy evaluation.

From this point, we propose a novel Variational Transformer (VaT) framework with both accuracy and diversity assurance programs. In specific, we first design an "Invisible Information Prior" (IIP) using unmasked input sentences to navigate the posterior encoder to learn the precise language attention map. Then we modify the single gaussian prior of VAE into an "Auto-selectable GMM" (AGMM) to fit the complex distribution of object relations in different scenes. IIP and AGMM form together to construct our assurance program for accuracy. Second, to ensure accuracy, Reinforce Learning (RL) is indispensable. Hence, we propose a reformulation of the self-critical sequence training (SCST) [5] employing a "Rang-Median Reward" (RMR) baseline to retain more diverse candidates with higher rewards during the RL training. Our Variational framework and RMR form together to construct our assurance program for diversity.

In this work, our main contributions are: **1)** We propose a novel model to promote accuracy and diversity at the same time, with 1.1 and 4.8 percent boost in accuracy (CIDEr) and diversity (self-CIDEr). **2)** We propose two assurance programs to make sure that our model generates diverse captions under a solid accuracy guidance. **3)** We also achieve the best trade-off performance in two newly proposed measurements, comparing with the human baseline (only 0.46 percent backward to the human-oriented boundary).

## 2 Related works

**Image captioning.** The most fundamental work in image captioning adopted the CNN-RNN-based Auto-Encoder (AE) structure as their backbone, including M-RNN [6], "Show and Tell" [7], and Deep Visual-Semantic Alignments [8]. Many follow-up efforts improve it with other technologies, like Attention Mechanism and Reinforcement Learning [9]. For example, [5, 10–13] applied different attention structures to simulate the human attention on both visual and language area; [14–17] utilized Reinforcement Learning algorithms to optimize the non-differentiable metrics, like CIDEr, directly on image captioning model; recently, [18, 19] introduced an external scene graph structure based on the human intuition when looking at a brief description to augment with the potential related attributes and objects, and even made it controllable to say as you wish.

**Improve accuracy with Attention and RL** Attention Mechanism is one of the most influential techniques to strengthen the accuracy performance. One representative is the "Bottom-Up and Top-Down" mechanism [10], which combined the attention mechanism in both vision and language area. As a vital derivative from Attention Mechanism, Transformer [20] plays an important role in image captioning in recent time, as it dramatically improves the accuracy performance. [12, 11, 13, 21] introduced several direct or related improvements to the basic Transformer model, while the purposes are similar, to intensify the ability of information filtration and multi-modal capacity.

Reinforce Learning is another important method to improve accuracy dramatically. [5] proposed the classic SCST strategy using greedy sampled sentences to refine the outputs with less diversity but better accuracy. Many works made modification based on this method, where the critical point lies in the baseline of RL training. [22, 16, 17] proposed three different and effective variants of RL baseline. We compared them with our RMR baseline to show our strength of improving diversity without damaging the accuracy performance.

**Improve diversity with VAE.** Variational Auto-Encoder [23] is wildly used in generative tasks, as well as several variants like CVAE [24] and [25] and beta-CVAE [26]. In image captioning, [27] proposed GMM-CVAE to estimate the KL-divergence between gaussian mixture distributions, using the extra object information from the detection model. In this work, we devised a similar AGMM variant that is trainable end-to-end and can better recognize object relations in different scenes. [28] is another exploration of Variational structure, which proposed a novel variational multi-modal inferring tree (similar to the syntax tree) to improve the lexical and syntactic diversity in captioning. At last, [4, 1] are two works which also concerned about the relation between accuracy and diversity like the main purpose of this work. [1] proposed an off-policy strategy to increase the range of samples during RL training, which improves the diversity dramatically, however, also causes the same dramatic decrease of accuracy. In our work, we fit this problem successfully through a well-designed framework.

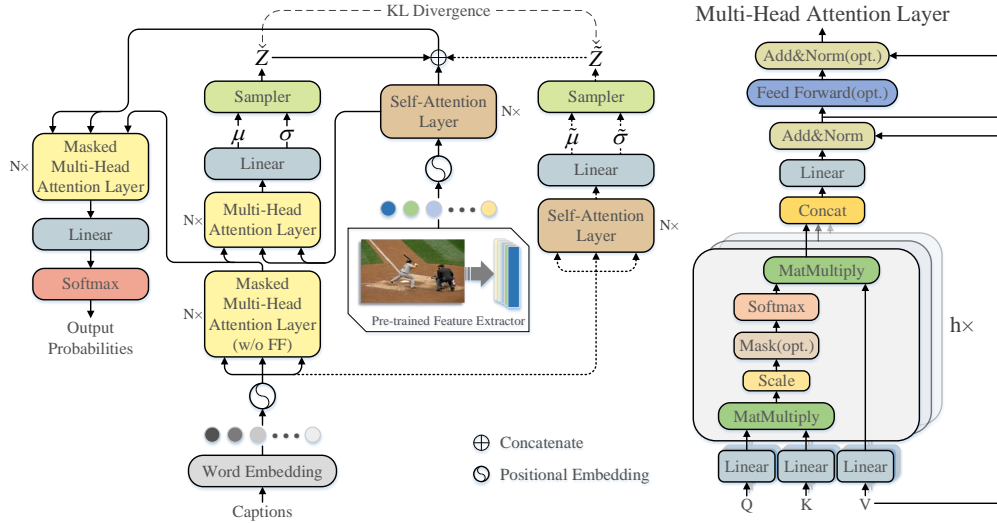


Figure 2: Overview of the proposed Variational Transformer architecture. The left figure shows the overall structure of our VaT model. The solid lines with the arrow present the inference route, while the dashed lines present the extra variational route at the training period. The right figure shows the specific Multi-Head Attention Layer in our model in contrast with the original Transformer Multi-Head Attention structure.

### 3 Variational Transformer

#### 3.1 Variational Auto Encoder

Typically, VAE theory was established on an assumption that the raw data points  $x$  cluster around a low-dimensional manifold parameterized by embeddings  $z$  [27]. Thus, we may rebuild  $x$  as long as we know the true distribution of  $z$ . The right side of the Equation (1) shows the Evidence Lower Bound (ELBO) on the log-likelihood of  $x$  in the vanilla VAE [23]. In the ideal case, we hope the distance between  $p$  and  $q$  to be minimized to 0. Hence, to maximize the objective likelihood of  $x$ , we only need to minimize the negative ELBO. However, the true distribution of  $z$  is rather difficult to discover with limited data sources. A conventional solution is to assume that the latent variable  $z$  behaves according to a given distribution, such as the standard normal distribution [23] or the gaussian mixture distribution [27].

$$\log p(x) - D_{\text{KL}} [q(z|x) \parallel p(z|x)] = \mathbb{E}_{q(z|x)} [\log p(x|z)] - D_{\text{KL}} [q(z|x) \parallel p(z)]. \quad (1)$$

Reviewing the ELBO in Equation (1), we found two specific optimization targets: the reconstructed log-likelihood of data point  $x$  and the KL divergence between the posterior  $q(z|x)$  and the prior  $p(z)$ . In common AE models, we only employ the log-likelihood as the reconstruction loss, while in VAEs, the KL divergence guides an extra variational route based on the normal AE structure. In our model, we utilize this route to introduce the “Invisible Information Prior”.

#### 3.2 Overall Framework

In our VaT model, several Attention Layers and Samplers are employed to establish the deterministic and stochastic connections between input series and output probabilities. In Figure 2, we have two different Attention Layers. For Self-Attention Layer, we retain the same structure of the original Transformer Encoder. For Multi-Head Attention Layer, we only make minor adjustments based on the original Transformer Multi-Head Attention module. In specific, we selectively compose the query searching, the residual structure and the feed forward module in the same layer for different parts, as shown in the right part of Figure 2. In the following, we will introduce how we design the variational route and utilize the invisible language information to navigate our VaT model to manage the “trade-off” conflict.

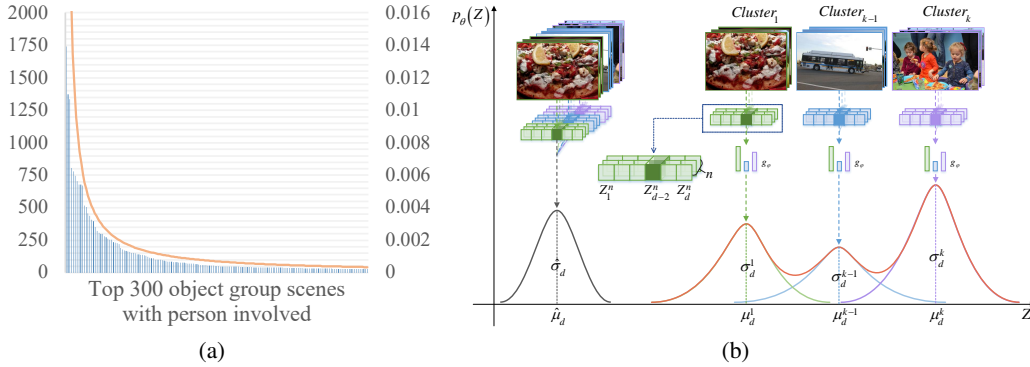


Figure 3: (a) Statistics of different object groups involving “person” in kaphaty’s test split. We choose the top 300 frequent groups to show the ratio of appearance. (b) Comparison between the single gaussian prior and our auto-selectable GMM.

**Invisible Information Prior.** The common language generation process employs a word-by-word pattern. For each timestep, the pdf of the current word  $x_t$  is based on the generated sentence fragment  $x_{<t}$ . As shown in Equation (1), each word can only see the previous sentence fragment, which is incomplete. This partial visible problem is essential and hard to find a solution under the common AE architecture, due to the lacking of ground truths at inference time. Therefore, we consider using VAE to make the information loss recuperated.

As introduced in Section 3.1, the normal variational process has an extra prior route during training period. This prior route gives the potential for VAE to introduce the invisible information when using the word-by-word generating pattern. To be specific, for each position of the latent variable  $z$ , we regard the full target sentence  $x$  as the prior information, meanwhile, regard the masked sentence  $x_{<t}$  and the image  $I$  as the posterior information to fit the generating pattern at inference time. Then we can reformulate the KL divergence of each position  $t$  into  $D_{\text{KL}}^t [q(z|x_{<t}, I) \parallel p(\tilde{z}|x)]$ . Under this alternation of target function, we will obtain a new variational route in our model, as shown in Figure 2. At training time, we use the prior  $\tilde{z}$  to decode the output probabilities for each word, while, at inference time, use  $z$  instead. To navigate the posterior encoder to learn the invisible language information from prior  $\tilde{z}$ , we follow the VAE theory to minimize the KL divergence between pdfs of  $z$  and  $\tilde{z}$ . Given an image  $I$ , we can draw the training target, i.e.,

$$L = -\mathbb{E}_{q_\phi(z|\tilde{x}, I)} [\log p_\theta(x|z, I)] + D_{\text{KL}} [q_\phi(z|\tilde{x}, I) \parallel p_\varphi(\tilde{z}|x)], \quad (2)$$

where  $\theta$ ,  $\phi$  and  $\varphi$  denote the parameters in different modules, and,

$$D_{\text{KL}} [q_\phi(z|\tilde{x}, I) \parallel p_\varphi(\tilde{z}|x)] = \frac{1}{T} \sum_{t=1}^T D_{\text{KL}}^t [q_\phi(z|x_{<t}, I) \parallel p_\varphi(\tilde{z}|x)]. \quad (3)$$

$T$  is the sequence length, and image  $I$  here in the posterior  $q_\phi(z|\tilde{x}, I)$  functions as a supplement for the posterior encoder to fill up the information loss caused by the fragmentary sentences.

### 3.3 Auto-selectable Gaussian Mixture Model

In the classic VAE theory, we use the standard normal distribution as the hypothetical prior. However, as shown in Figure 3(b), using single gaussian is trying to embed the information of the entire set of images into one tuple of parameter  $(\mu, \sigma)$  for each dimension of  $z$ . This will, intuitively and practically, reserve much noisy information due to the indiscriminate embedding of images, meanwhile, raise a mismatch between the data distribution and the hypothesis prior. To overcome this problem, [27] proposed a GMM-based CVAE model, in which the kernel of GMM was manually selected according to the object detection results of each image. This pattern has two issues. First, the capacity of GMM depends on the efficiency of the pre-trained detection model. Second, the same object in different scenes will share the same kernel in GMM, thus, have the same mean and variance. In another words, these objects with distinct semantic information will share the same latent representation.

As shown in Figure 3(a), we counted different object groups with “person” involved in the training set and illustrate the top 300 groups’ frequency. It behaves as a long-tailed distribution, which means, we could embed the major information for one object appeared in different scenes with a feasible kernel number. But the selection of each kernel should rely on the semantic level (dimension level) instead of the object level (one kernel for one object). Therefore, we designed a novel GMM selection principal that can automatically match the object and its latent representation in different scenes using a simple learnable parameter  $g_\varphi$ . In specific, we choose the kernel for each dimension of  $z$  according to the prior kernel probability  $\omega = \text{softmax}(g_\varphi)$ . Technically, each dimension of  $z$  will get a chance to fit the corresponding part of information into each kernel without force of mixture.

Given the auto-selection principle in Figure 3(b), we follow the upper bound in [29] and make some slight modifications to turn it trainable end-to-end. Firstly, we consider  $p$  and  $q$  to be GMMs that have the same number of components  $K$ . The marginal densities of  $x \in \mathbb{R}^d$  under  $p$  and  $q$  can be expressed as Equation 4.

$$p(x) = \sum_{k=1}^K \omega_k \mathcal{N}(x; \mu_k; \Sigma_k),$$

$$q(x) = \sum_{k=1}^K \tilde{\omega}_k \mathcal{N}(x; \tilde{\mu}_k; \tilde{\Sigma}_k),$$
(4)

where  $\omega_k$  and  $\tilde{\omega}_k$  are the prior probabilities of each component in  $p$  and  $q$ .  $\mathcal{N}(x; \mu; \Sigma)$  is a gaussian in  $x$  with mean  $\mu$  and covariance  $\Sigma$ . Then under the chain rule of relative entropy [30], we have the following upper bound.

$$D_{\text{KL}}(p||q) \leq D_{\text{KL}}(\omega||\tilde{\omega}) + \sum_{k=1}^K \omega_k D_{\text{KL}}(p_k||q_k)$$

$$= \sum_{k=1}^K \omega_k \log \frac{\omega_k}{\tilde{\omega}_k} + \sum_{k=1}^K \omega_k D_{\text{KL}}(p_k||q_k).$$
(5)

This upper bound can be further minimized by searching for the optimized mapping relation between the components of  $p$  and  $q$ , but the searching process is too expensive for the deep learning model. Consequently, we replace the KL-divergence in Equation 2 with this practicable upper bound and reform our training target as:

$$L_{\text{vat}} = -\mathbb{E}_{q_\phi} [\log p_\theta(x|z, I)] + \beta * \sum_{k=1}^K \omega_k \left( \log \frac{\omega_k}{\tilde{\omega}_k} + D_{\text{KL}}[q_{\phi_k} || p_{\varphi_k}] \right),$$
(6)

where  $\beta$  is the coefficient to adjust the ability of the proposed disentanglement theory [26]. Through this reformulation, we can transform the calculation of the KL-divergence between GMMs into the calculation between each component of GMMs. Especially when we let every components in the upper bound 5 have the same prior probabilities as  $\frac{1}{K}$ , it will be equivalent to the expectation of the KL-divergence between each component pair, like the implementation in [27].

### 3.4 Range-Median Reward Baseline

Like we have discussed in Section 1, unilaterally improving diversity is insufficient for generating human-like captions. RL training is essential to guarantee the accuracy performance. The policy gradient of SCST shows in Equation 7, where  $\hat{x} = (\hat{x}_1, \dots, \hat{x}_T)$ ,  $\hat{x}_t$  is the word sampled from the model at sequence position  $t$ , and  $b$  is the greedy search baseline. This form introduces a better gradient variance reduction compared with the general cross-entropy loss. To achieve a further improvement reducing the variance, [22] replaced the greedy sampled baseline  $b$  with the average score of the rest sampled candidates. For  $n$ th sample,  $b_{\text{avg}}(\hat{x}_n) = \mathbb{E}_{j \neq n} r(\hat{x}_j)$ . This

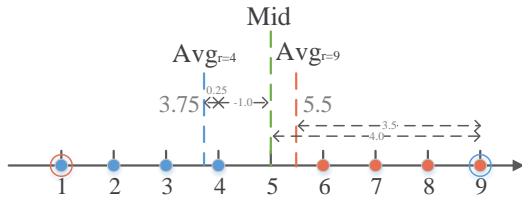


Figure 4: Intuitive analysis for different reinforce learning baselines.

simple change can effectively improve the accuracy performance. However, as indicated by [1], SCST encourages the samples with higher scores to be more likely sampled along with the training progressed, which inevitably causes the diversity performance reduction. Even for our VaT model, using SCST will take a toll on the diversity performance. Therefore, we proposed a novel baseline using the Range Median of all samples to improve the diversity without sacrificing the accuracy when adopting SCST method.

$$\nabla_{\theta} \approx - (r(\hat{x}) - b) \nabla_{\theta} \log p_{\theta}(\hat{x}|z, I), \quad (7)$$

We give an extreme case in Figure 4, where the blue and orange circles indicate two groups of reward scores that have four close rewards and one outlier in each. We denote this two groups with  $s_1 = \{1, 2, 3, 4, 9\}$  and  $s_2 = \{1, 6, 7, 8, 9\}$ . The green dashed line indicates our Range-Median Reward (RMR) baseline. The calculation formula shows in Equation 8.

$$b_{mid}(\hat{x}) = \left( \max_{\hat{x}_n \in \hat{X}} (r(\hat{x}_n)) + \min_{\hat{x}_n \in \hat{X}} (r(\hat{x}_n)) \right) / 2 \quad (8)$$

In our formula, we consider the global information of all samples’ rewards. For example in group  $s_1$ , we have an extreme high score 9. In the average baseline, the reward for the sample 4 will be 0.25, which encourages the sample with a low score. Meanwhile, in our median baseline, the reward for the sample 4 decreases to  $-1.0$ , which properly punished the low-scored sample. Similarly, we will get a encouragement for sample 6 in  $s_2$  using our median baseline, while the average baseline will punish it. In this way, our median baseline reserves more positive samples with higher scores to improve the valid diversity performance instead keeping the false inferences for irrationally increasing the diversity metrics scores without considering the semantic accuracy.

Another advantage of our median baseline is that the intensity of encouragement and penalty will increase compared with the average pattern. In  $s_2$ , the rewards for the sample 9 are 4.0 and 3.5 using median and average baseline, respectively. Likewise, samples with low scores in  $s_1$  will get intensive punishment using our median baseline.

At last, we should note that, for the sample groups that have a balance distribution, our median baseline and the average baseline are less differentiating especially in the last stage of SCST training. The experimental results illustrate that our median baseline can get a fair accuracy performance compared with the average pattern, meanwhile, obtain a higher diversity performance.

## 4 Evaluation

### 4.1 Dataset and evaluation metrics

**Dataset** We evaluate our model on the most popular benchmark MSCOCO [31] in the image captioning area. For consensus comparison, we adopt the Karpathy’s split [8], which contains 113, 287 images for training, 5, 000 for validation and external 5, 000 for testing. Each image in the split is associated with at least five manual captions.

**Accuracy metrics** In our experiments, we follow the most popular AE methods to impose several metrics evaluate the quality of accuracy in contrast with the human captions, including BLEU [32], METEOR [33], ROUGE [34], CIDEr [35], and SPICE [36].

**Diversity metrics** For diversity evaluation, we adopt five benchmark diversity metrics in [27, 28, 4, 1]. 1) *n-gram diversity* (Div-n): the ratio of distinct n-grams to the total number of words in the generated captions. Higher score of Div-n is better. 2) *mean Bleu-N* (mB-N): the mean value of the Bleu-N scores that are calculated between each caption in a set of K captions against the rest K-1 ones. It measures the inner similarities between the generated caption samples. Lower is better. 3) *Unique Sentence Ratio* (Uni.): the average ratio of distinct sentences in sampled sets. Higher is better. 4) *self-CIDEr* (S-C): singular vector decomposition (SVD) over autocorrelation matrices of the generated caption set using CIDEr as the kernel. Higher is better. 5) *AllSPICE* (All.): the F-score in a single scene graph for the generated caption set, that SPICE treats the same way with the reference caption sets. Higher is better with a balanced performance of accuracy and diversity.

Table 1: Ablation study results on COCO Karpathy test split. Accuracy metrics: B- $N$ , M, R, C, and S represent BLEU@ $N$ , METEOR, ROUGE-L, CIDEr, and SPICE. Diversity metrics: Uni., Div- $N$ , mB- $N$ , and All. represent Unique Sentence Ratio, n-gram diversity, mean BLEU- $N$ , and AllSPICE. "↓" denotes that the lower score is better. All results are reported in percentage(%).

Optimization target	Models	Accuracy						Diversity					Accuracy promoted (average)	Diversity promoted (average)	
		B-1	B-4	M	R	C	S	Uni.	All.	Div-1	Div-2	mB-4 ↓			S-C
CE	Transformer(baseline)	75.6	35.8	27.9	56.4	114.0	<b>21.1</b>	99.9	22.3	55.7	75.6	17.8	89.8	-	-
	VaT <sub>GMM1</sub>	75.9	<b>35.9</b>	27.9	56.5	113.7	20.8	100.0	22.1	<b>59.2</b>	<b>79.6</b>	<b>12.4</b>	<b>92.0</b>	-	✓
	VaT <sub>AGMM32</sub>	<b>76.2</b>	35.8	<b>27.9</b>	<b>56.5</b>	<b>114.4</b>	20.8	<b>100.0</b>	<b>22.4</b>	58.6	79.3	12.6	91.8	✓	✓
CE+NSC	Transformer(baseline)	80.8	39.2	29.0	58.8	130.1	22.7	54.6	25.3	22.6	27.6	89.0	38.5	-	-
	VaT <sub>GMM1</sub>	80.7	39.4	28.9	58.8	129.3	22.6	<b>73.9</b>	<b>26.8</b>	<b>26.8</b>	<b>34.6</b>	<b>79.9</b>	<b>46.8</b>	-	✓
	VaT <sub>AGMM32</sub>	<b>80.9</b>	<b>39.8</b>	<b>29.2</b>	<b>59.0</b>	<b>131.2</b>	<b>23.1</b>	70.1	26.6	25.4	32.9	82.3	43.3	✓	✓
CE+MSC	Transformer(baseline)	80.7	39.1	29.0	58.8	130.1	22.8	63.1	26.0	24.0	30.3	85.6	37.3	-	-
	VaT <sub>GMM1</sub>	80.8	39.5	28.9	58.8	129.9	22.7	70.5	26.3	25.7	33.4	85.4	44.1	-	✓
	VaT <sub>AGMM32</sub>	<b>81.2</b>	<b>39.7</b>	<b>29.1</b>	<b>59.0</b>	<b>130.3</b>	<b>23.0</b>	<b>71.5</b>	<b>26.8</b>	<b>25.9</b>	<b>33.8</b>	<b>81.0</b>	<b>44.9</b>	✓	✓

## 4.2 Implementation details

**Image Feature Extractor** To obtain the precise features corresponding to the ROIs under the guidance of Attention Mechanism, we follow the Updown method in [10] to use the pre-trained object features as image representation. For every image, we use a finetuned Faster R-CNN [37] with Resnet-101 [38], annotated and trained on the Visual Genome dataset [10, 39], to detect 10-100 regions (adaptive) and extract the corresponding features with 2048 dimensions. All the image features are pre-extracted as provided in [10, 15].

**Experiment Settings** We set the batch size to 10 in all our experiments for consensus. The number of layer was set to 4, the inner-dimension  $d$  as well as the dimension of the latent variable  $z$  was set to 512, and the dimension of the feedforward layer was 1024. For every latent  $z$  we set the number of GMM kernel to 32. We trained our model with Adam optimization [40] and the Reduce-LR-On-Plateau method for learning rate decay at every validation step. For initialization, we set the learning rate to  $1 \times 10^{-4}$ , the patience steps of decay to 3, and the coefficient  $\beta$  to 1.0. The training process endured 30 epochs including 15 for the cross-entropy training and another 15 for the self-critical training (using CIDEr optimization). Our project can be found on github <sup>1</sup>.

## 4.3 Ablation Study

To prove the effectiveness of our VaT framework and IIP module, we use the original Transformer in [20] as our baseline and follow its hyperparameter settings. To prove the effectiveness of our AGMM and RMR module, we use the single gaussian prior and the average reward RL baseline [22] as the contrast, separately. All models in our ablation experiments share the same hyperparameter settings and training strategy. In table 1, we present both accuracy and diversity performance of different contrast models. CE, NSC and MSC indicate the cross entropy loss, the average self-critical optimization in [22] and our RMR method, respectively. The subscript GMM $N$  indicates that the model uses the GMM prior with  $N$  kernels. We mark the best scores in bold and the second with the underline.

Under the same experiment conditions, our VaT framework using AGMM with 32 kernels outperforms the Transformer baseline and simultaneously promotes the accuracy and diversity. Meanwhile, using the single gaussian prior can only promote diversity, as other diverse models do. Furthermore, experiments under NSC and MSC optimization illustrate that our RMR baseline maintains a better diversity performance without sacrificing the accuracy capacity (prevent the normal trade-off costs), especially when the trade-off gap is extremely exhibited by using the self-critical optimization.

Table 2: Accuracy performance on COCO Karpathy test split, comparing with the state-of-the-art methods. All results are reported in percentage(%).

Models	Year	B-1	B-4	M	R	C	S
Att2in* [5]	2017	78.4	35.7	27.3	56.9	119.5	20.7
UpDown* [10]	2018	79.9	37.1	28.0	57.8	123.8	21.5
AoA* [11]	2019	80.3	38.3	28.7	58.4	127.0	22.3
SGAE [19]	2019	80.8	38.4	28.4	58.6	127.8	22.1
Transformer*	-	80.8	39.2	29.0	58.8	130.1	22.7
M2Transformer* [12]	2020	80.7	39.1	29.0	58.8	129.0	22.7
B-SCST [16]	2020	80.8	39.0	29.2	59.0	131.0	22.9
APN [21]	2021	-	39.6	29.2	<b>59.1</b>	<b>131.8</b>	23.0
MAC [13]	2021	<b>81.5</b>	39.5	<b>29.3</b>	58.9	131.6	22.8
TRRL [17]	2021	<u>81.4</u>	39.2	28.5	59.0	128.7	22.0
VaT <sub>msc</sub> (ours)	-	81.2	<u>39.7</u>	29.1	59.0	130.3	<u>23.0</u>
VaT <sub>nsc</sub> (ours)	-	80.9	<b>39.8</b>	<u>29.2</u>	<u>59.0</u>	131.2	<b>23.1</b>

<sup>1</sup><https://github.com/kaelsunkiller/VaT>

#### 4.4 Evaluating the Accuracy Performance

In Table 2, we introduce several state-of-the-art accurate methods, mainly including those based on the Transformer structure or similar attention oriented structures. Results from these methods with the superscript \* are reproduced under Luo’s code framework <sup>2</sup>, while others without \* are all quoted directly from the original papers. All models are trained with the self-critical optimization. Our model get a similar performance comparing with accurate models, especially when they are usually bad at generating diverse captions. In Section 4.5, We will show that our model performs outstandingly not only in accuracy evaluation but in diversity evaluation as well.

#### 4.5 Evaluating the Diversity performance associated with accuracy metrics

Table 3 summarizes the diversity performance of different accurate and diverse models. We evaluate the diversity performance associated with the accuracy metrics to ensure that our model produces better diverse captions along with a solid accuracy performance. For consensus evaluation, all results of comparison methods are reported after the self-critical training. For multiple captions sampling, we employ the diverse sampling [3] with  $\lambda = 0.5$ .

First, we compare our model with AE models that have a better accuracy performance. Results suggest that our model outperforms others in both accuracy and diversity. Especially, we have achieved 44.9 in self-CIDEr using the RMR baseline with 6.5 percent promotion compared with the best of AE models.

Second, we compare our model with generative models that aim to promote the diversity. Note that we report the result of our model using CE optimization due to the inevitable diversity damage caused by the self-critical training. Curiously, our model outperforms not only the other diverse models but also the leave-one-out results of human [2]. Is that an evidence that our model generates better captions than human? Unfortunately, it is not. Actually, with CE optimization, most accurate models are able to provide better metric results than human’s (leave-one-out). Naive Transformer gets 114.0 in CIDEr and 89.8 in self-CIDEr, for example. However, as we have indicated in Section 1, higher metric scores not consistently represent a better performance, a better diversity performance must establish on a solid accuracy performance to generate truly human-like captions. Then, how to measure the benefits of each model? In Section 4.6, we propose a simple method to calculate model’s capability of holding the diversity under a consensus criteria of accuracy.

#### 4.6 Analysing the trade-off gap with human performance

In order to generate diverse captions under the bondage of semantic accuracy, the self-critical training must be involved. Yet, the gap of accuracy between diverse models and accurate models becomes an intractable heterogeneity. To solve this problem, we need a consistent reference value, in which the margin of "trade-off" can be borrowed. From this conception, we introduce a simple measurement to calculate the "trade-off" using human performance as the reference.

$$TPR(a, b) = \frac{1}{2} \left( \frac{Acc_a - Acc_b}{Acc_b} + \frac{Div_a - Div_b}{Div_b} \right) \quad (9)$$

Equation 9 is the formulation of our compounded Trade-off Profit Rate (TPR), where a can be models we aim to assess, b is the baseline. In this function, we consider both increase or decrease of accuracy and diversity correlated to human performance. According to the trade-off phenomenon, with one item (accuracy or diversity) increases, another (diversity or accuracy) generally decreases. TPR calculates the compounded promotion rate within the trade-off margin. In our experiments, we use leave-one-out captions of human as b, CIDEr as *Acc* and self-CIDEr as *Div*.

<sup>2</sup><https://github.com/ruotianluo/self-critical.pytorch>

Table 3: Diversity performance of different models correlated to accuracy metrics. All results are reported in percentage(%).

Models	Accuracy			Diversity		
	B-4	M	C	Uni.	mB-4 ↓	S-C
Accurate Models						
Att2im* [5]	35.7	27.3	119.5	51.8	90.6	27.3
UpDown* [10]	37.1	28.0	123.8	56.5	89.0	31.9
AoA* [11]	38.3	28.7	127.0	57.8	89.0	32.4
Transformer*	39.2	29.0	130.1	54.6	89.0	38.5
M2Transformer* [12]	39.1	29.0	129.0	63.7	85.4	38.2
VaT <sub>msc</sub> (ours)	<u>39.7</u>	<u>29.1</u>	<u>130.3</u>	<b>71.5</b>	<b>81.0</b>	<b>44.9</b>
VaT <sub>nsc</sub> (ours)	<b>39.8</b>	<b>29.2</b>	<b>131.2</b>	<u>70.1</u>	<u>82.3</u>	<u>43.3</u>
Diverse models						
GMM-CVAE [27]	18.9	21.7	78.5	90.9	45.6	70.7
CapGAN [41]	15.8	22.1	68.7	78.0	76.9	59.0
Off-Policy [1] ( $\epsilon = 0.1$ )	26.5	24.5	89.9	92.0	54.0	69.3
Off-Policy [1] ( $\epsilon = 0.9$ )	15.0	19.9	57.3	99.6	27.3	80.6
VaT <sub>cc</sub> (ours)	<b>35.8</b>	<b>27.9</b>	<b>114.4</b>	<b>100.0</b>	<b>12.6</b>	<b>91.8</b>
Human (leave-one-out)	19.5	24.1	87.8	100.0	19.5	88.6



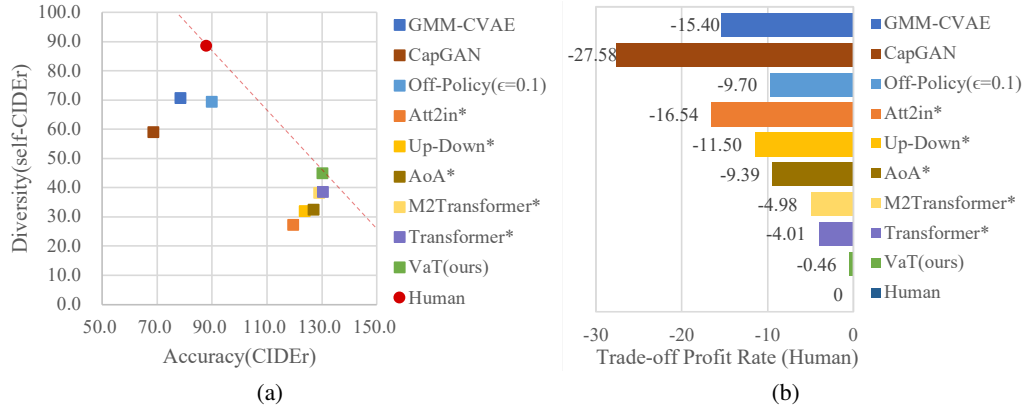
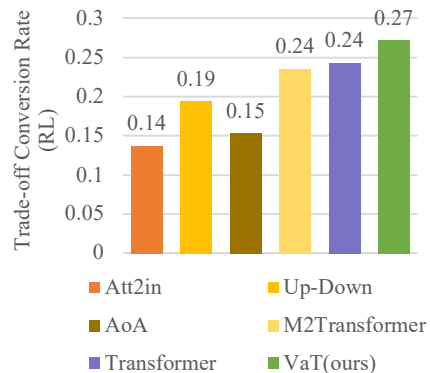


Figure 5: Trade-off analysis of different works. (a) Performance of different works associated with both accuracy and diversity. The dashed line represent the zero TPR bound correlated to the human performance. (b) Relative Trade-off profit of each work. Our model achieves the closest result to human performance. All results are reported in percentage(%).

In Figure 5(a), we demonstrate the performance of different works associated with both accuracy and diversity performance. The red dashed line is the zero bound of  $TPR_{human}$ , where for every point on the line  $TPR(\text{point}, \text{human}) = 0$ . Our model locates closest to this bound, which indicates that our model achieves almost the same rate of accuracy promotion as the diversity consume. In Figure 5(b) we report the specific TPR scores of each work. We are the closest one to the human standard with the solid accuracy performance.

$$TCR_{RL} = \left( \frac{|Div_{CE} - Div_{RL}|}{Div_{RL}} \right) / \left( \frac{|Acc_{CE} - Acc_{RL}|}{Acc_{RL}} \right) \quad (10)$$

We also designed another variant of TPR, for evaluating the trade-off in RL training, i.e. Trade-off Conversion Rate (TCR). This perception is derived from the energy conversion efficiency (ECE):  $\eta = P_{out}/P_{in}$ . In our scenario, RL training can be considered as the machine that converse the input power (diversity) to the output power (accuracy). According to this concept, we built TCR to measure the trade-off efficiency of RL training for different methods. As shown in Figure 6, our model achieves the best conversion performance.



#### 4.7 Qualitative analysis

Due to the page limit, we put the qualitative analysis in Supplemental Material, Appendix A.

Figure 6: Trade-off conversion rate of different works.

## 5 Conclusion

In this work, we propose a novel framework consist of different well-designed modules to ensure the diverse generation with the accurate semantic structure. First, we give the group of IIP and AGMM to guarantee the accuracy performance. Then, we give the RMR baseline to improve the quality of diverse generation based on a solid accuracy foundation. Extensive experiments suggest that our model achieves a simultaneous promotion in both accuracy and diversity. Furthermore, to evaluate the overall performance under the trade-off phenomenon, we propose two simple measurements to calculate the compounded trade-off rate. Also, we get the closest performance to the human-oriented zero profit bound.

## References

- [1] J. Shi, Y. Li, and S. Wang, “Partial off-policy learning: Balance accuracy and diversity for human-oriented image captioning,” in *Proceedings of the IEEE conference on computer vision and pattern recognition*, 2021, pp. 2187–2196.
- [2] Q. Wang and A. B. Chan, “Describing like humans: on diversity in image captioning,” in *Proceedings of the IEEE conference on computer vision and pattern recognition*, 2019, pp. 4195–4203.
- [3] A. K. Vijayakumar, M. Cogswell, R. R. Selvaraju, Q. Sun, S. Lee, D. Crandall, and D. Batra, “Diverse beam search: Decoding diverse solutions from neural sequence models,” *arXiv preprint arXiv:1610.02424*, 2016.
- [4] R. Luo and G. Shakhnarovich, “Analysis of diversity-accuracy tradeoff in image captioning,” *arXiv preprint arXiv:2002.11848*, 2020.
- [5] S. J. Rennie, E. Marcheret, Y. Mroueh, J. Ross, and V. Goel, “Self-critical sequence training for image captioning,” in *Proceedings of the IEEE conference on computer vision and pattern recognition*, 2017, pp. 7008–7024.
- [6] J. Mao, W. Xu, Y. Yang, J. Wang, Z. Huang, and A. Yuille, “Deep captioning with multimodal recurrent neural networks (m-rnn),” *arXiv preprint arXiv:1412.6632*, 2014.
- [7] O. Vinyals, A. Toshev, S. Bengio, and D. Erhan, “Show and tell: A neural image caption generator,” in *Proceedings of the IEEE conference on computer vision and pattern recognition*, 2015, pp. 3156–3164.
- [8] A. Karpathy and L. Fei-Fei, “Deep visual-semantic alignments for generating image descriptions,” in *Proceedings of the IEEE conference on computer vision and pattern recognition*, 2015, pp. 3128–3137.
- [9] R. S. Sutton and A. G. Barto, *Reinforcement learning: An introduction*. MIT press, 2018.
- [10] P. Anderson, X. He, C. Buehler, D. Teney, M. Johnson, S. Gould, and L. Zhang, “Bottom-up and top-down attention for image captioning and visual question answering,” in *Proceedings of the IEEE conference on computer vision and pattern recognition*, 2018, pp. 6077–6086.
- [11] L. Huang, W. Wang, J. Chen, and X.-Y. Wei, “Attention on attention for image captioning,” in *Proceedings of the IEEE/CVF International Conference on Computer Vision*, 2019, pp. 4634–4643.
- [12] M. Cornia, M. Stefanini, L. Baraldi, and R. Cucchiara, “Meshed-memory transformer for image captioning,” in *Proceedings of the IEEE conference on computer vision and pattern recognition*, 2020, pp. 10 578–10 587.
- [13] J. Ji, Y. Luo, X. Sun, F. Chen, G. Luo, Y. Wu, Y. Gao, and R. Ji, “Improving image captioning by leveraging intra-and inter-layer global representation in transformer network,” in *Proceedings of the AAAI Conference on Artificial Intelligence*, vol. 35, no. 2, 2021, pp. 1655–1663.
- [14] M. Ranzato, S. Chopra, M. Auli, and W. Zaremba, “Sequence level training with recurrent neural networks,” *arXiv preprint arXiv:1511.06732*, 2015.
- [15] R. Luo, B. Price, S. Cohen, and G. Shakhnarovich, “Discriminability objective for training descriptive captions,” in *Proceedings of the IEEE conference on computer vision and pattern recognition*, 2018, pp. 6964–6974.
- [16] S. Bujimalla, M. Subedar, and O. Tickoo, “B-scst: bayesian self-critical sequence training for image captioning,” *arXiv preprint arXiv:2004.02435*, 2020.
- [17] W. Nie, J. Li, N. Xu, A.-A. Liu, X. Li, and Y. Zhang, “Triangle-reward reinforcement learning: A visual-linguistic semantic alignment for image captioning,” in *Proceedings of the 29th ACM International Conference on Multimedia*, 2021, pp. 4510–4518.
- [18] S. Chen, Q. Jin, P. Wang, and Q. Wu, “Say as you wish: Fine-grained control of image caption generation with abstract scene graphs,” in *Proceedings of the IEEE conference on computer vision and pattern recognition*, 2020, pp. 9962–9971.
- [19] X. Yang, K. Tang, H. Zhang, and J. Cai, “Auto-encoding scene graphs for image captioning,” in *Proceedings of the IEEE conference on computer vision and pattern recognition*, 2019, pp. 10 685–10 694.
- [20] A. Vaswani, N. Shazeer, N. Parmar, J. Uszkoreit, L. Jones, A. N. Gomez, Ł. Kaiser, and I. Polosukhin, “Attention is all you need,” *Advances in neural information processing systems*, vol. 30, 2017.

- [21] X. Yang, C. Gao, H. Zhang, and J. Cai, "Auto-parsing network for image captioning and visual question answering," in *Proceedings of the IEEE conference on computer vision and pattern recognition*, 2021, pp. 2197–2207.
- [22] R. Luo, "A better variant of self-critical sequence training," *arXiv preprint arXiv:2003.09971*, 2020.
- [23] D. P. Kingma and M. Welling, "Auto-encoding variational bayes," in *International conference on learning representations*, 2014.
- [24] D. P. Kingma, S. Mohamed, D. Jimenez Rezende, and M. Welling, "Semi-supervised learning with deep generative models," *Advances in neural information processing systems*, vol. 27, 2014.
- [25] K. Sohn, H. Lee, and X. Yan, "Learning structured output representation using deep conditional generative models," *Advances in neural information processing systems*, vol. 28, 2015.
- [26] I. Higgins, L. Matthey, A. Pal, C. P. Burgess, X. Glorot, M. Botvinick, S. Mohamed, and A. Lerchner, "beta-vaе: Learning basic visual concepts with a constrained variational framework," in *International conference on learning representations*, 2017.
- [27] L. Wang, A. Schwing, and S. Lazebnik, "Diverse and accurate image description using a variational auto-encoder with an additive gaussian encoding space," *Advances in Neural Information Processing Systems*, vol. 30, 2017.
- [28] F. Chen, R. Ji, J. Ji, X. Sun, B. Zhang, X. Ge, Y. Wu, F. Huang, and Y. Wang, "Variational structured semantic inference for diverse image captioning," *Advances in Neural Information Processing Systems*, vol. 32, 2019.
- [29] J. R. Hershey and P. A. Olsen, "Approximating the kullback leibler divergence between gaussian mixture models," in *2007 IEEE International Conference on Acoustics, Speech and Signal Processing-ICASSP'07*, vol. 4. IEEE, 2007, pp. IV–317.
- [30] T. M. Cover, *Elements of information theory*. John Wiley & Sons, 1999.
- [31] T.-Y. Lin, M. Maire, S. Belongie, J. Hays, P. Perona, D. Ramanan, P. Dollár, and C. L. Zitnick, "Microsoft coco: Common objects in context," in *European conference on computer vision*. Springer, 2014, pp. 740–755.
- [32] K. Papineni, S. Roukos, T. Ward, and W.-J. Zhu, "Bleu: a method for automatic evaluation of machine translation," in *Proceedings of the 40th annual meeting of the Association for Computational Linguistics*, 2002, pp. 311–318.
- [33] M. Denkowski and A. Lavie, "Meteor universal: Language specific translation evaluation for any target language," in *Proceedings of the ninth workshop on statistical machine translation*, 2014, pp. 376–380.
- [34] C.-Y. Lin, "Rouge: A package for automatic evaluation of summaries," in *Text summarization branches out*, 2004, pp. 74–81.
- [35] R. Vedantam, C. Lawrence Zitnick, and D. Parikh, "Cider: Consensus-based image description evaluation," in *Proceedings of the IEEE conference on computer vision and pattern recognition*, 2015, pp. 4566–4575.
- [36] P. Anderson, B. Fernando, M. Johnson, and S. Gould, "Spice: Semantic propositional image caption evaluation," in *European conference on computer vision*. Springer, 2016, pp. 382–398.
- [37] S. Ren, K. He, R. Girshick, and J. Sun, "Faster r-cnn: Towards real-time object detection with region proposal networks," *Advances in neural information processing systems*, vol. 28, 2015.
- [38] K. He, X. Zhang, S. Ren, and J. Sun, "Deep residual learning for image recognition," in *Proceedings of the IEEE conference on computer vision and pattern recognition*, 2016, pp. 770–778.
- [39] R. Krishna, Y. Zhu, O. Groth, J. Johnson, K. Hata, J. Kravitz, S. Chen, Y. Kalantidis, L.-J. Li, D. A. Shamma *et al.*, "Visual genome: Connecting language and vision using crowdsourced dense image annotations," *International journal of computer vision*, vol. 123, no. 1, pp. 32–73, 2017.
- [40] D. P. Kingma and J. Ba, "Adam: A method for stochastic optimization," *arXiv preprint arXiv:1412.6980*, 2014.
- [41] R. Shetty, M. Rohrbach, L. Anne Hendricks, M. Fritz, and B. Schiele, "Speaking the same language: Matching machine to human captions by adversarial training," in *Proceedings of the IEEE International Conference on Computer Vision*, 2017, pp. 4135–4144.